Production regimes in the northeast Atlantic: A study based on Sea-viewing Wide Field-of-view Sensor (SeaWiFS) chlorophyll and ocean general circulation model mixed layer depth

Marina Lévy,[1] Yoav Lehahn,[1,2] Jean-Michel André,[3] Laurent Mémery,[4] Hubert Loisel,[5] and Eyal Heifetz[2]

Received 15 October 2004; revised 31 January 2005; accepted 6 April 2005; published 20 July 2005.

[1] A 5 year time series of Sea-viewing Wide Field-of-view Sensor (SeaWiFS) ocean color images (SCHL) is compared with mixed layer depths (MLD) and atmospheric forcings from the Clipper model of the North Atlantic (1998–2002). This comparison is done over the region 16°–22°W, 30°–50°N, where subpolar mode waters are formed and which overlaps the region of the 2001 Programme Océan Multidisciplinaire Méso Echelle (POMME) experiment at sea. Three production regimes are identified on the basis of the seasonal cycling of SCHL and MLD: the well-known subpolar and subtropical regimes and a midlatitude regime. The midlatitude regime is characterized by a single broad bloom weaker than the subpolar spring bloom and stronger than the subtropical fall bloom, which starts in fall as an entrainment bloom and peaks in spring as a restratification bloom. This specific regime is found between 35°N and 40°N (±2°) in the northeast Atlantic. It corresponds to winter MLDs between *Ze* (the depth of the euphotic layer) and 2*Ze*, i.e., it lays between the region where the winter MLD is greater than Sverdrup's critical depth (subpolar regime) and the region where the mixing is never deeper than the well-lit layer (subtropical regime). The very specific characteristics of the midlatitude regime strengthen the biological carbon pump since production is active in winter within the waters to be subducted. The midlatitude regime also may provide an explanation for the unexpectedly low *f* ratios sometimes observed during the bloom in the region (North Atlantic Bloom Experiment, POMME). A large interannual variability is observed for the three regimes in terms of the timing and the intensity of the blooms and of the geographical boundaries of the regimes. These variabilities appear to be mainly driven by the synoptic and the low-frequency atmospheric variabilities. It is also shown that in addition to the northward propagation of the subpolar spring bloom from 41°N (±1.3°) to 50°N, the (fall) entrainment bloom propagates southward over the whole latitudinal range (35°–50°N).

Citation: Lévy, M., Y. Lehahn, J.-M. André, L. Mémery, H. Loisel, and E. Heifetz (2005), Production regimes in the northeast Atlantic: A study based on Sea-viewing Wide Field-of-view Sensor (SeaWiFS) chlorophyll and ocean general circulation model mixed layer depth, *J. Geophys. Res.*, *110*, C07S10, doi:10.1029/2004JC002771.

1. Introduction

[2] In the northeast Atlantic, the spring bloom and the formation of subpolar mode waters occur during the same period. Subpolar mode waters, characterized by a low potential vorticity and a temperature between 11° and 12°C, are subducted at the end of winter [*Woods*, 1985]. The intensity of the bloom and the exact timings of bloom and subduction play major roles in setting the biogeochemical characteristics of the water masses that will be isolated for a decade from the influence of the atmosphere, and therefore on the efficiency of the physical and biological carbon pumps. The Programme Océan Multidisciplinaire Méso Echelle (POMME) research project was designed to achieve a better understanding of the coupling between the dynamical processes involved in subduction and the biological processes involved in the oceanic carbon cycle [*Mémery et al.*, 2005]. Field experiments were carried out over a seasonal cycle, from October 2000 to October 2001. The area of interest extends zonally from 16°W to 22°W and meridionally from 38°N to 45°N (Figure 1). This area

[1]Institut Pierre-Simon Laplace, Centre National de Recherche Scientifique, Paris, France.
[2]Geophysics and Planetary Sciences, Tel Aviv University, Tel Aviv, Israel.
[3]Institut Pierre-Simon Laplace/Institut de Recherche Pour le Développment, Paris, France.
[4]Laboratoire des Sciences de l'Environnement Marin/Institut Universitaire Européen de la Mer, Centre National de Recherche Scientifique, Plouzané France.
[5]Laboratoire d'Optique Atmosphérique, Universite des Sciences et Technologies de Lille, Villeneuve d'Ascq, France.

0148-0227/05/2004JC002771$09.00

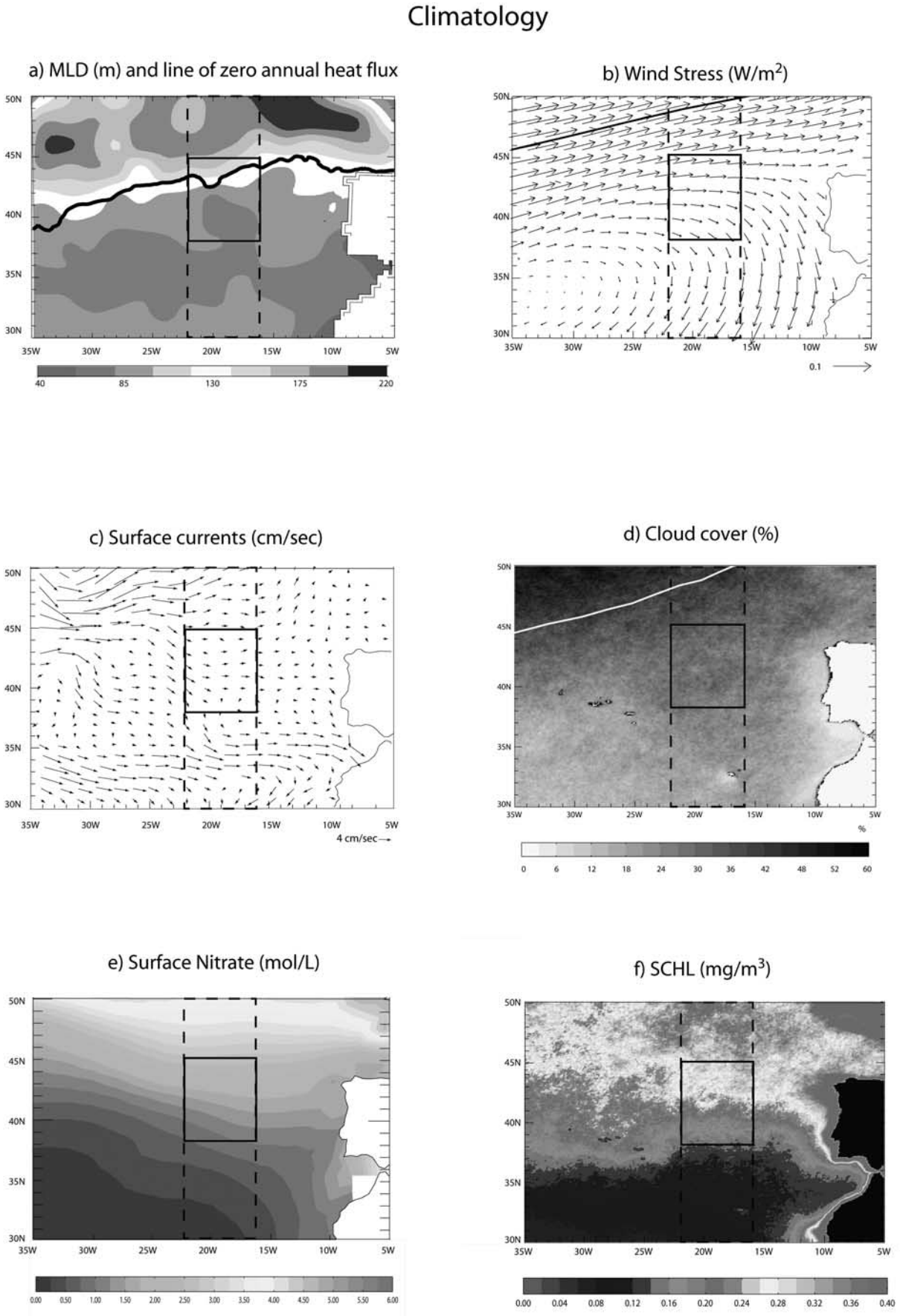
Climatology
a) MLD (m) and line of zero annual heat flux
50N
45N
40N
35N
30N
35W 30W 25W 20W 15W 10W 5W
40 85 130 175 220
b) Wind Stress (W/m2)
0.1
c) Surface currents (cm/sec)
4 cm/sec
d) Cloud cover (%)
%
0 6 12 18 24 30 36 42 48 52 60
e) Surface Nitrate (mol/L)
0.00 0.50 1.00 1.50 2.00 2.50 3.00 3.50 4.00 4.50 5.00 5.50 6.00
f) SCHL (mg/m3)
0.00 0.04 0.08 0.12 0.16 0.20 0.24 0.28 0.32 0.36 0.40

Figure 1

corresponds to a transition zone between a productive region in the north, associated with quite deep late winter mixed layers (200–300 m), and an oligotrophic region in the south, associated with relatively shallow (100 m) winter mixed layers [*Sathyendranath et al.*, 1995]. Both regions are characterized by a pronounced seasonal cycle, and an important year to year variability [*Stramska et al.*, 1995; *Michaels and Knap*, 1996; *Williams et al.*, 2000; *Dutkiewicz et al.*, 2001; *Follows and Dutkiewicz*, 2002; *McClain et al.*, 2004; *Dandonneau et al.*, 2004]. Estimates of surface ocean chlorophyll (SCHL) from space provide an opportunity to reveal this variability more clearly on a synoptic scale over several years.

[3] This study focuses on SCHL as detected by SeaWiFS over the region 16°–22°W, 30°–50°N from 1998 to 2002, where subpolar mode waters are formed and which overlaps the region of the 2001 POMME experiment. It is aimed at explaining aspects of the seasonal cyclings and interannual changes in terms of mixed layer depth (MLD) behavior and meteorological forcing. This analysis is conducted with particular emphasis on the timing of the spring bloom and of subduction. Variability of the bloom in terms of timing, intensity, intermittency, duration and propagation is discussed with respect to three specific biogeochemical regimes, which will be identified in the data set: the well-known subpolar and subtropical regimes and a midlatitude regime. The study insists on the midlatitude regime (found between 35°N and 40°N ± 2° in the northeast Atlantic and corresponding to winter MLDs comprising between *Ze*, the depth of the euphotic layer, and 2*Ze*), due to its important role in the Atlantic carbon pump. A special attention is also paid to the analysis of the seasonal cycling in 2001, the POMME year, and the synoptic view of the system during the cruises.

[4] Our approach is guided by previous studies on SCHL variability in the region. Phytoplankton growth involves a balance between nutrient supply and light forcing. The deepening of the oceanic mixed layer (ML) supplies nutrients while decreasing the averaged light level experienced by the phytoplankton population. The interplay between these two competing effects has been rationalized by *Dutkiewicz et al.* [2001]. They identify two regimes based on the ratio of the spring critical depth to the MLD at the end of winter: anomalously high spring mixing decreases SCHL in the subpolar regime, and enhances SCHL in the subtropical regime. This classification is based on *Sverdrup*'s [1953] critical depth theory and on *Menzel and Ryther* [1961] observations that in the Sargasso Sea the bloom generally occurs when the ML is at its deepest. By applying *Dutkiewicz et al.* [2001] concepts to SeaWiFS time series observations binned into 5° × 5° regions in conjunction with reanalyzed NCEP meteorological data, *Follows and Dutkiewicz* [2002] show that the expected SCHL-to-mixing relationships emerge in both regimes. In this low-resolution study, no clear trend emerges in the POMME region which appears as a transition between the two regimes. Besides, the POMME region overlays the flanks of the subtropical gyre where *Williams and Follows* [1998] modeling study suggests that productivity is controlled by an Ekman injection of nitrogen from the north. However, by combining climatological nitrate profiles with MLD cycles and wind stress data, *Williams et al.* [2000] found that the interannual variability in nitrate supply is largely controlled by convection rather than by Ekman transfer and that the largest interannual variability in convective nitrate supplies occurs in the POMME area. *Bograd et al.* [2004] used SeaWiFS data to study the annual migration of the chlorophyll front in the transition zone of the north Pacific. They found significant interannual variations in the front location which they attributed to wind changes through a combination of two processes: changes in the wind stress curl which influences the redistribution of nutrients in the surface waters through Ekman horizontal divergence, and changes in the wind intensity which acts to mix nutrients up to the surface. The position of the boundary between the eutrophic regime in the north and the oligotrophic regime in the south of the POMME region is very likely to be affected by the same processes.

[5] We combine 5 years of SeaWiFS data with MLDs, heat fluxes and wind stresses derived from general circulation models of the ocean and atmosphere. Section 2 details the methodology. Climatological patterns, seasonal and interannual variability of the different fields are successively presented in section 3 with emphasis on their meridional structures. These variabilities are discussed in section 4 before the study is given a conclusion.

2. Data and Methods

[6] The analysis of the spatio-temporal variability is based on time series of satellite images and model outputs that are now described.

2.1. Satellite-Derived Chlorophyll

[7] SCHL estimates are derived from SeaWiFS. They are representative of the phytoplankton pigment concentration within the mixed layer [e.g., *André*, 1992]. We used the Level 3 (9 km) weekly composites from the Distributed Active Archive Center of the Goddard Earth Sciences (GES-DAAC) at NASA after reprocessing #4. The data set corresponds to the period from January 1998 to December 2002. The accuracy of satellite retrieval over the POMME region was estimated by comparing satellite estimates of SCHL with coincident (in time and space) in

Figure 1. A climatological view of the northeast Atlantic. (a) Winter mixed layer depth (MLD) (after *de Boyer Montegut et al.* [2004]) and the line of zero annual net heat flux in Clipper between the years 1998 and 2002. (b) Wind stress (European Centre for Medium-Range Weather Forecasts (ECMWF)) and line of zero wind stress curl. (c) Surface currents (after *Paillet and Mercier* [1997]). (d) Cloud cover as percent of flag occurrence over 1998–2002 in Sea-viewing Wide Field-of-view Sensor (SeaWiFS) weekly chlorophyll products (see text) and the line of 50% cloud cover. (e) Surface nitrate [*Levitus*, 1982]. (f) Surface chlorophyll (average of SeaWiFS ocean color images (SCHL) over 1998–2002). The solid frame marks the Programme Océan Multidisciplinaire Méso Echelle (POMME) region, and the dashed frame marks the region examined in the present study. See color version of this figure at back of this issue.

situ measurements during POMME. The estimated ratio of satellite-to-in-situ SCHL is 1.06 ± 0.28%, i.e., no significant bias and a small standard deviation (more details will be available in the work of H. Loisel et al. (manuscript in preparation, 2005)). Level 3 weekly composites are significantly cloudy for the north Atlantic in winter. An average cloud cover was computed as the percentage of masking occurrence for each pixel over the 5 years. Very high SCHL were often observed in the vicinity of clouds. After examination of in situ regional measurements, values greater than 5 mg/m^3 were considered as unrealistic and were filtered out.

2.2. Model Products

[8] The evolutions of the MLD and of the net heat flux are derived from the ATL6 Clipper simulation of the North Atlantic (described in detail by *Tréguier et al.* [2003]). This simulation was performed with the primitive equation model OPA [*Madec et al.*, 1999] in a domain that covers the Atlantic Ocean from 75°S to 70°N with a horizontal resolution of 1/6°. Vertical resolution is 12 m at the surface and decreases to 200 m below 1550 m. The model is forced with the daily ECMWF analysis from 1979 to 2002. The heat forcing is corrected by applying a relaxation of SST toward Reynolds satellite data. In this paper, the net heat flux is defined as the sum of the ECMWF analysis heat flux and of this correction term. Wind stress is from ECMWF analysis. Clipper outputs are 5 day averages.

[9] MLD is diagnosed as the depth at which the density differs from its surface value by 0.05 kg/m3. In order to evaluate the quality of the Clipper MLDs, they have been compared to the MLDs predicted by three other models and with POMME data. The results of this comparison will be discussed in section 4.

2.3. Analysis of the Variability

[10] Our analysis of the SCHL variability relies on comparisons with the MLD. We examine three scales of variability. We start with an overview of the main large-scale climatological patterns over the northeast Atlantic (5°–35°W, 30°–50°N). This meridional extension covers significant parts of the southern oligotrophic region and of the northern productive region, as well as the transition region in between. In a second stage, we examine the seasonal cycling of SCHL and MLD from September 2000 to October 2001 (the period of the POMME experiment) and restrict our analysis to the zonal extent of the POMME region (16°–22°W). When computing zonal averages, this range is large enough to counterbalance the relatively large cloud cover. In a third stage, we analyze the interannual variations of the coupled cycles between 1998 and 2002.

[11] In order to derive the bloom onset and the bloom duration, a low-pass time filter is applied to the satellite time series. This allows to retain only the seasonal signal and to remove sources of variability due to higher frequencies. The bloom onset is an important parameter whose determination has been designed according to the bloom dynamics. In particular, two dynamics of bloom onset were observed (see later) which called for specific criteria. For sharp SCHL rises following fast ML retreats (spring blooms), the onset is defined as the time of SCHL maximum derivative (maximum growth). For mild SCHL increases driven by slow ML deepenings (entrainment blooms), the onset is defined as the time of SCHL zero derivative (beginning of growth). In both cases, the end of the bloom is defined as the time when the SCHL comes back to its onset value. The propagation speed of the bloom onset is computed as the time derivative of its location, averaged over the latitude range of the propagation. Finally, the bloom strength is defined as the average SCHL over the duration of the bloom.

3. Results

3.1. Climatological Patterns

[12] A central feature of the northeast Atlantic is the sharp transition between the area of deep winter MLDs in the north, and shallower MLDs in the south [*Arhan et al.*, 1994; *Paillet and Arhan*, 1996a]. Figure 1a shows how clearly this emerges in the recent climatology of *de Boyer Montégut et al.* [2004]; in February, MLDs reach 220m in the north and 100m in the south. The strongest winter MLD gradient (located around 43°N) is aligned with the line of zero annual net heat flux. This gradient is mostly meridional, although the front is slightly inclined from southwest to northeast due to the presence of the North Atlantic Current (NAC) in the northwest (Figure 1c). Besides the NAC, the geostrophic circulation at the surface, as reconstructed from an inverse model by *Paillet and Mercier* [1997], reveals a strong eastward current farther south (around 33°N), known as the Azores Current (AC). Two branches of southward recirculation appear along 30°W and 22°W. These branches are connected with the AC in the south. Surface winds are generally directed eastward (Figure 1b), and rotate from northeastward at 50°N to southeastward at 35°N. The zero wind stress curl is located at around 45°N and slightly inclined (Figure 1b). The resulting Ekman transport is directed southward and associated with upwelling in the northern subpolar gyre and downwelling in the southern subtropical gyre [e.g., *Williams and Follows*, 1998; *Williams et al.*, 2000]. It is the combination of the winter meridional MLD gradient with the weak southward circulation which leads to the subduction of subpolar mode water [*Paillet and Arhan*, 1996a, 1996b]. Subduction occurs when the mixed layer retreats and it is maximum over the area of maximum MLD gradient [*Marshall et al.*, 1993; *Hazeleger and Drijfhout*, 2000; *Valdivieso da Costa et al.*, 2005].

[13] In the SeaWiFS climatology (Figure 1f), the two well-known productivity regimes of the north Atlantic appear. The north is productive with high mean values of SCHL (>0.4 mg/m^3), and the south is oligotrophic with low mean SCHL values (<0.1 mg/m^3). This spatial structure is the result of the meridional variations in the distribution of nutrients (Figure 1e) resulting itself from the physical forcings structure (see above). In the north, deep winter mixed layers allow high rates of convective supply of nutrients to the euphotic layer [*Williams et al.*, 2000]. This, together with the upwelling of nutrient rich water and the raising of the thermocline by the gyre circulation enables an efficient phytoplankton growth and the region is relatively productive. In the south, the opposite scenario of downwelling from a shallow mixed layer is found and the region is oligotrophic [*Williams and Follows*, 2003]. Cloud cover increases with latitude, from 10% south of 35°N to more

than 60% north of 50°N (Figure 1d). In the region of the POMME experiment, the cloud cover ranges between 20% and 40%.

[14] To sum up, the POMME region is characterized by relatively weak currents, small zonal variability and strong meridional gradients. The area is split by the lines of zero annual net heat flux, zero wind stress curl, maximum MLD and SCHL gradients.

3.2. Seasonal Cycling (September 2000–October 2001, the Year of the POMME Experiment)

[15] The period from September 2000 to October 2001 is used to identify the main features of the seasonal cycling. Besides their seasonal variations, all parameters exhibit high-frequency signals. The timing and intensity of the high-frequency events vary from one year to another. They will be specifically described for the POMME year.

3.2.1. Production Regimes

[16] The zonal character of most features in the climatologies (Figure 1) drives to focus on meridional and temporal variations. Zonal averages, as presented in Figure 2, reveal the expected strong seasonality of all fields.

[17] The net heat flux (Qnet) switches from negative to positive values around March, and becomes negative again during September (Figure 2a). The timing of the zero Qnet varies with latitude: warming occurs earlier in the south (in spring) and cooling occurs earlier in the north (in fall), both by about 1 month between 30°N and 50°N. Qnet is also strongly modulated by the occurrence of wind bursts, which are frequent in autumn and winter, particularly north of 40°N (Figure 2b). In the northeast Atlantic, the ML variability is essentially driven by Qnet. When Qnet is positive, the ocean warms up, the water column stratifies and the ML shallows. When Qnet is negative, static instabilities are generated and convection deepens the ML. Over the whole latitude range examined, the ML is thus forced to deepen in fall (earlier in the north) and to shoal in spring (earlier in the south (Figure 2c)). Vertical mixing generated by strong wind events drive short-term ML variability that can prevail over a stabilizing effect of Qnet; an example is the ML deepening event at the end of P2L2 (strong wind and positive Qnet at the beginning of May).

[18] The seasonality of SCHL is driven by the seasonality of the atmospheric forcing, in particular through the solar flux and the MLD variations. The seasonal cycling of SCHL changes with latitude (Figure 2d). This meridional change results from much deeper winter MLDs in the north than in the south (300 m versus 120 m, as predicted by the Clipper model).

[19] In the north (north of 40°N on the 2001 picture), the main features are a major bloom in spring (''subpolar spring bloom'') and a relatively small bloom in autumn (thereafter ''subpolar fall bloom''). In summer, production is nutrient limited over most of the region and SCHL are small; the subsequent subpolar fall bloom is a response to the nutrient entrainment driven by the deepening of the mixed layer. The fall bloom lasts as long as phytoplankton is retained within the well-lit layer; it ends in winter when the ML becomes deeper than Sverdrup's critical depth. Incidentally, the minimum SCHL in summer is not as marked north of 49°N; at these latitudes light levels are likely too low to force a full consumption of the available nutrients in summer. During the northern winter, production is inhibited by too deep a mixing and the subpolar spring bloom is triggered by the restratification of the water column. As it appears in Figure 2, the period of highest biomass closely follows the period of deepest ML.

[20] In the south (south of 35°N on the 2001 picture), the SCHL signal is characterized by a single weak bloom that starts in the fall and reaches its peak in February. As the fall bloom of the subpolar regime, this ''subtropical (fall) bloom'' is an entrainment bloom [*Michaels et al.*, 1996], initiated by a deepening of the mixed layer. In contrast to what happens in the northern winter, the southern ML does not deepen beyond a critical threshold; the subtropical bloom ends with the exhaustion of nutrients [*Fernández et al.*, 2005], and not because the ML becomes too deep. It appears in Figure 2 that the period of highest biomass matches rather closely the period of deepest ML.

[21] At midlatitudes (between 35°N and 40°N on the 2001 picture), SCHL appears to follow a seasonal cycling in relation to the MLD cycling which differs markedly from the typical subpolar and subtropical cyclings. The SCHL signal is characterized by a single broad bloom of intermediate amplitude, weaker than the subpolar spring bloom and stronger than the subpolar and subtropical fall blooms. This single bloom begins at fall with the deepening of the ML, which is characteristic of an entrainment bloom (as in both the subtropical and subpolar regimes) and keeps developing in winter. It reaches its peak in spring, after restratification, which is characteristic of a spring bloom (as in the subpolar regime). Figure 2d might give the impression of a progressive evolution from the subtropical regime to the subpolar regime. However, we believe that a third specific regime emerges from this analysis, a ''midlatitude regime.'' This midlatitude regime is characterized by the merging of a fall bloom with a spring bloom. The midlatitude bloom is both light and nutrient limited, contrary to the spring bloom which is essentially light limited, and to the entrainment blooms which are essentially nutrient limited. Specific criterion can be drawn to identify the midlatitude regime. First, the absence/presence of a fall bloom enables to distinguish between the midlatitude and the subpolar regimes. Second, the midlatitude and subtropical regimes differ in the dynamics of their single bloom. In the subtropical regime, nutrient limitation prevails; when nutrients are provided by the deepening of the ML, the bloom proceeds at high efficiency. This results in the peak of the bloom occurring simultaneously or slightly before the maximum MLD. In the midlatitude regime, phytoplankton is both light and nutrient limited; when the ML deepens, nutrient limitation decreases but light limitation increases. The bloom starts at a slow rate. Only when the ML shallows again does the bloom reach its maximum efficiency. This is characterized by the peak of the bloom occurring after the maximum MLD. The midlatitude regime has specific biogeochemical implications, which will be discussed farther.

[22] To make the picture clearer, the 2001 SCHL and MLD seasonal cycles have been averaged for the 3 specific regimes, i.e., for this particular year, over the 30°–35°N, 35°–40°N and 40°–45°N latitude bands. After filtering out high-frequency variability, they are plotted in Figure 3. As shown by the paired curves, the ''midlatitude bloom'' starts as a fall bloom and switches to a spring bloom. It lasts

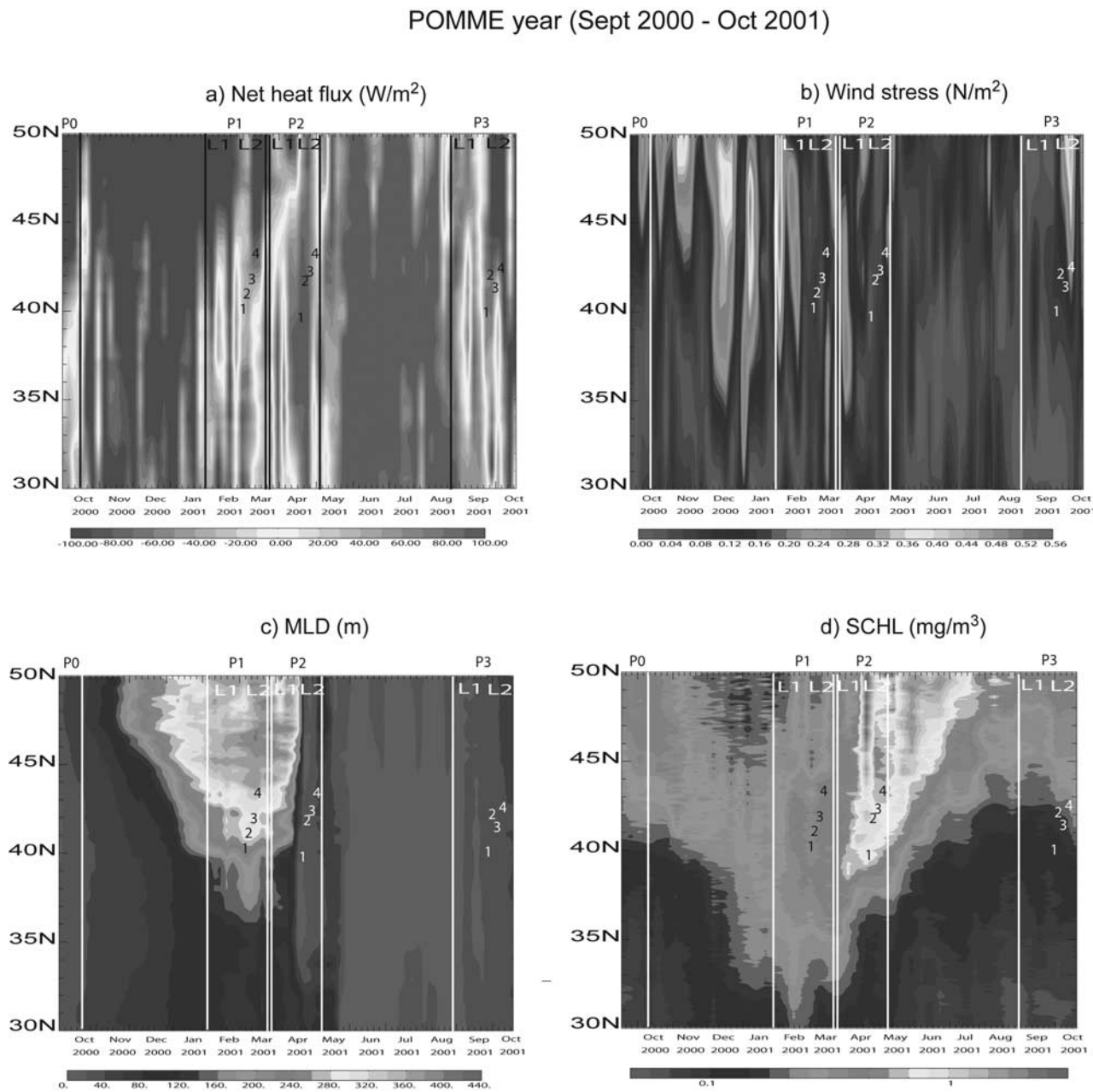

Figure 2. Temporal and meridional variations of zonal averages (16°–22°W) from September 2000 to October 2001 of (a) net heat flux (Clipper), (b) wind stress (ECMWF), (c) MLD (Clipper), and (d) SCHL (SeaWiFS). The vertical lines mark the period of each POMME survey (P0 to P3). The numbers mark the location and time of the time series stations. Legs 1 (L1) and 2 (L2) of each survey are also indicated. See color version of this figure at back of this issue.

longer than the other blooms. Its amplitude is intermediate between that of the subpolar spring bloom and that of the subpolar and subtropical fall blooms. The time shift between maximum MLD and maximum SCHL is also intermediate between that for the subtropical bloom and that for the subpolar spring bloom. Section 3.3 will provide further assessment of the 3 regimes.

3.2.2. Focus on the POMME Cruises

[23] From September 2000 to October 2001, four POMME cruises took place. The first cruise (P0) was conducted in September 2000. The most complete coverage occurred during P1 (February–March 2001) and P2 (March–May 2001). The last cruise P3 occurred in late August–early October, 1 year after P0 (vertical white lines on Figure 2 indicate the first and last date of each cruise). The cruises were usually divided into two legs. The first legs (L1 on Figure 2) were dedicated to a large-scale survey of the area [*Mémery et al.*, 2005]. The main study area (39°–44.5°N, 16°–21°W) was covered with 7 latitudinal transects, with CTD stations approximately 50 km apart and basic JGOFS type of measurements (nutrients, oxygen, inorganic and organic carbon, phytoplankton, primary pro-

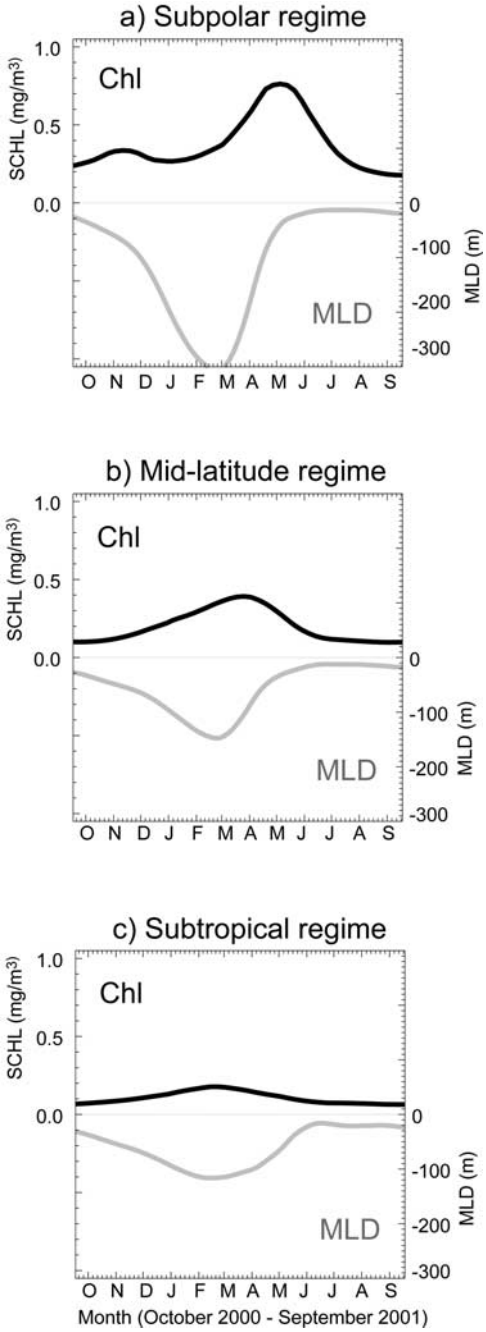

Figure 3. Time evolution from September 2000 to October 2001 of zonal averages (16°–22°W) of SCHL (black lines) and MLD (shaded lines) in (a) the subpolar region (meridionally averaged between 40° and 45°N), (b) the midlatitude region (35°–40°N), and (c) the subtropical region (30°–35°N). The signals are smoothed by convolution with a 120 day window.

duction, bio-optical observations, etc.). This coverage lasted around 3 weeks. During the second legs (L2), four time series stations (numbered 1 to 4 on Figure 2) were carried out to investigate 1D biogeochemical processes. They generally lasted 2 days. A complete set of physical, chemical and biological parameters were measured in specific regions of the mesoscale field to give information on the mesoscale dynamics, on the mixed layer evolution, on the biogeochemical stocks and fluxes and on the ecosystem structure [*Mémery et al.*, 2005]. The aim of P1 was to describe the winter conditions in order to estimate the maximum MLD and set the initial prebloom conditions. The spring cruise P2 immediately followed, with the objective of characterizing the mode waters and the bloom evolution. The aim of P3 was to capture oligotrophic conditions. POMME in situ data were used to validate the SCHL and MLD used in this work (see sections 2.1 and 4.1).

[24] A drawback of POMME observational strategy is the strong asynopticity in the data [*Lévy et al.*, 2005]. Particularly during the bloom, the duration of the first leg is long compared to the characteristic timescales of the weather, of the MLD and of the ecosystem. During the second legs, it is again difficult to determine if the biogeochemical differences observed from one station to another are due to their specific location, to the progression along the seasonal cycle or to a response to different local weather conditions.

[25] SeaWiFS data provide a synoptic view that enables us to situate these four POMME cruises within the seasonal cycle and the series of wind events. Figure 2d reveals very clearly that P0 occurred during the 2000 fall bloom. P1 was initially planned to represent winter preconditioning conditions. SeaWiFS data reveal that this winter regime was actually reached prior to P1, between P0 and P1. P1 appears as a period of slow growth: the ML is at its maximum depth. Between 35°N and 40°N, P1 covers the beginning of the midlatitude bloom, i.e., the period during which it has the characteristics of an entrainment bloom. Growth is accelerated during two short periods of fine weather, one during P1-L1, and the other during P1-L2 (stations 3 and 4). Maximum SCHL values are reached during P2; the second part of the midlatitude bloom (spring bloom type) occurs during P2. The wind event in May occurs during the end of P2, and causes dilution of phytoplankton at P2 time series stations 3 and 4. P3 appears as a typical summer oligotrophic regime, close to equilibrium, and ends with the 2001 fall bloom.

[26] This 2001 example shows that the seasonal cycle is perturbed by synoptic atmospheric events. These can either accelerate (as in mid-February) or decelerate (as in the beginning of May) phytoplankton growth. It is noteworthy that these high-frequency events spotted in totally independent data sets (ECMWF and SeaWiFS) are remarkably in phase.

3.3. Variability Over the 5 Years

[27] In order to examine how the seasonal cycling changes with latitude throughout the 5 years, SCHL and MLD were averaged zonally between 16°W to 22°W and meridionally in 1° bands from 30°N to 46°N. The resulting seasonal cycles are presented in Figure 4. For each situation (year and 1° latitude band), the paired SCHL and MLD curves were compared to the three ''models'' of production regime proposed in Figure 3. Each situation was determined to belong to one of the three specific regimes on the basis of objective criteria. More precisely, the boundary between the subpolar and the midlatitude regime was defined as the latitude at which the fall bloom merges with the spring bloom. A smoothing was applied to the SCHL curves to

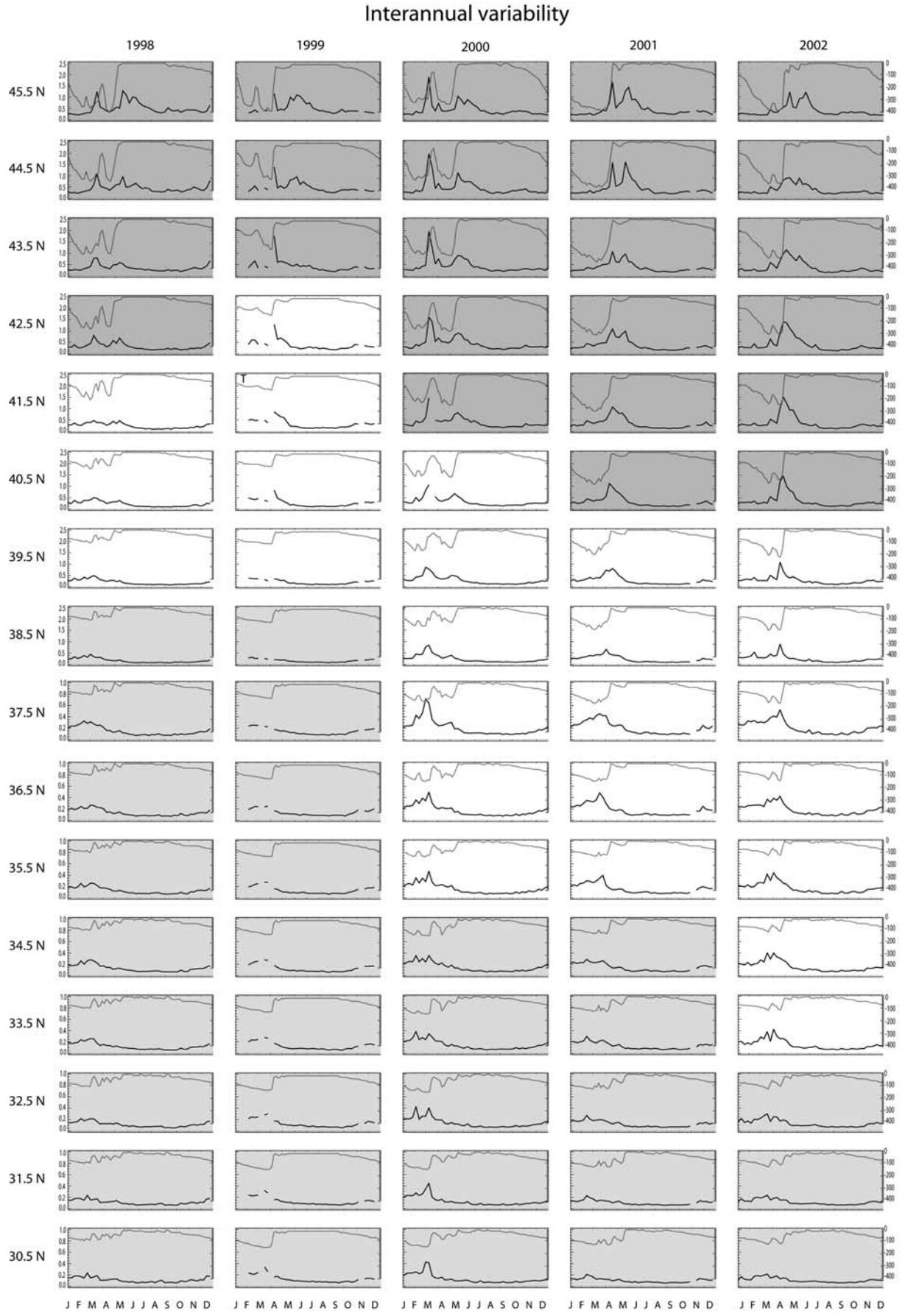
Interannual variability
1998
1999
2000
2001
2002
45.5 N
44.5 N
43.5 N
42.5 N
41.5 N
40.5 N
39.5 N
38.5 N
37.5 N
36.5 N
35.5 N
34.5 N
33.5 N
32.5 N
31.5 N
30.5 N
J F M A M J J A S O N D

Figure 4

remove high-frequency variability. Smoothed SCHL curves where a local minimum (in summer) was found in between two local maxima (in autumn and spring) were assigned to the subpolar regime. The boundary between the midlatitude and the subtropical regime was determined on a criterion involving the timing of the maximum MLD versus the timing of the maximum SCHL peak. Situations where the SCHL peak followed the MLD peak were assigned to the midlatitude regime, and inversely situations where the SCHL peak preceded or was simultaneous to the MLD peak were assigned to the subtropical regime. According to these criteria, seasonal cycles of subpolar type were marked in Figure 4 with a dark shaded background, midlatitude ones with white and subtropical ones with light shading.

3.3.1. General Features

[28] On the basis of Figure 4, we now describe the features of the three regimes that are consistent throughout the 5 years and the features that vary.

[29] In the subpolar regime, the maximum MLD is always greater than 250 m. The spring bloom is characterized by an abrupt increase in SCHL in response to a rapid shoaling of the ML. The bloom develops at the end of the stratification transition and its intensity is always higher than 1 mg/m^3. Beside the spring bloom, a fall bloom occurs in all of the situations in Figure 4. Driven by the ML deepening after the summer minimum, the fall bloom reaches its peak (of the order of 0.5 mg/m^3) well before the end of the winter deepening.

[30] In the subtropical regime, the maximum MLD is always less than 120m. There is always a single and relatively weak fall bloom, driven by the ML deepening of the mixed layer. The biomass peaks at less than 0.4 mg/m^3 at about the same time as the MLD reaches its maximum.

[31] In the midlatitudes regime, the maximum MLD comprises between 120 m and 250 m. There is always a single bloom. Its intensity ranges between the maximum value encountered for the subtropical fall bloom (0.4 mg/m^3) and the minimum value observed for the subpolar spring bloom (1 mg/m^3). The midlatitude bloom peaks during the shoaling phases of the mixed layer and lasts longer than the blooms in the two other regimes.

[32] As regards the timing of the blooms, Figure 4 shows significant variability within the latitude range, as well as from one year to the next. For the subpolar spring bloom, the onset occurs earlier in the south and varies with an overall amplitude of almost 5 months. For the subpolar fall bloom, the onset (generally in August–September) occurs earlier in the north and varies with an overall amplitude of 2 months. It is exceptionally late in 1998 (late October). The midlatitude (fall) bloom onset (most generally in September–October) also occurs earlier in the north and the overall amplitude of its meridional/interannual change is of the order of 2 months. It is exceptionally late in 1998 (early November). The timing of the subtropical bloom (onset always in November) also occurs earlier in the north but the overall variation of the onset is of the order of only 1 month.

[33] The SCHL maximum is highly variable from one year to the next. In the subpolar regime, it does not exceed much 1 mg/m^3 in 1998 and 1999 but reaches 1.5 to 1.8 mg/m^3 in some of the 2000, 2001 and 2002 situations. It is worth noting that, for each of the 5 years, the bloom is not a smooth SCHL variation: most generally it is briefly interrupted by a sudden redeepening of the ML, to resume with the definite seasonal restratification. As regards the subpolar fall bloom, its peak ranges from a minimum value of about 0.5 mg/m^3 in 2002 to a maximum of about 0.7 mg/m^3 in 1998. In the midlatitude regime, the bloom peak ranges from a minimum value of around 0.5 mg/m^3 (encountered over the whole region in 1998 and in its southern part for all years) to a maximum of around 1 mg/m^3 (encountered in the northern part of the region in 1999, 2000 and 2002). The midlatitude bloom is most generally characterized by a single peak. Exceptionally, in 2000, an event of redeepening during the ML shoaling period leads to a secondary SCHL peak. In the subtropical regime, the (fall) bloom shows a lesser variability in its intensity, with an annual peak generally between 0.21 mg/m^3 and 0.27 mg/m^3. An exception is the bloom of 1999–2000, with two strong peaks at about 0.4 mg/m^3. It is also worth noting that both the MLD and SCHL signals exhibit a rather moderate variability at high frequency, compared with the two other regimes.

[34] The location of the regimes boundaries changes significantly from one year to another. The southern boundary of the subpolar regime is at 42°–43°N at the beginning of the time series in 1998–1999 and shifts toward 40°N at the end in 2002. For the northern boundary of the subtropical regime, the meridional shift over the 5 years is from 39°N to 33°N. The meridional extension of the midlatitude regime thus varies from a minimum of 3° in 1998 to a maximum of 7° in 2002. The amplitude of the interannual variation of the southern boundary is approximately twice as large as for the northern limit.

3.3.2. Physical Interpretation

3.3.2.1. Bloom Onset and Propagation

[35] The information about the variations of the bloom onset has been synthesized in Figure 5. The well-known northward "propagation" of the subpolar spring bloom is shown in Figure 5a. Interestingly, a southward propagation is also evidenced. This southward propagation concerns the entrainment bloom, i.e., the succession from north to south of the subpolar fall bloom, the midlatitude bloom and the subtropical bloom. When looking at the *y-t* SCHL representation (Figure 2d), the impression is of a northward propagation over the whole latitudinal range, i.e., from 30°N to 50°N. This northward propagation (Figure 2d) is that of the SCHL peak; it is reached in March in the subtropics, in April at midlatitudes and in May in the north. The peak marks the beginning of the decline of the bloom, and this northward propagation (already observed by, e.g., *Yoder et al.* [1993], *Siegel et al.* [2002], *Follows and Dutkiewicz* [2002], and *Dandonneau et al.* [2004]), likely reflects the meridional gradient in nutrient limitation rather

Figure 4. Seasonal cycles of SCHL (black lines) and MLD (shaded lines) averaged zonally between 16° and 22°W and meridionally over 1° stripes between 30° and 46°N. The dark shaded, light shaded, and white backgrounds mark the subpolar, oligotrophic, and midlatitudes regimes, respectively. Note the change in the SCHL scale north and south of 38°N.

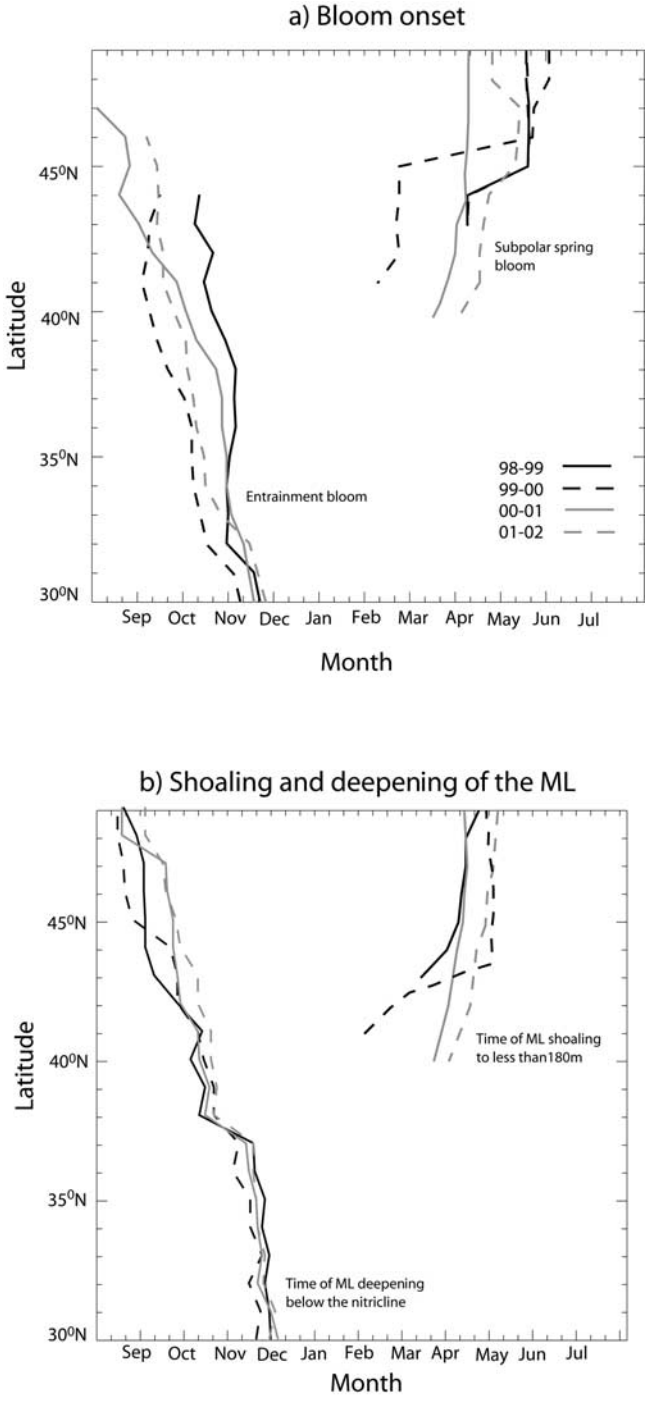

Figure 5. For each year and as a function of latitude, (a) the onset time of the various blooms and (b) the time when the ML deepens below the fall nitracline and the time when it shallows above 180 m.

than the northward propagation in irradiance: nutrients being more abundant in the north, their exhaustion last longer. In our analysis, we are dealing with the propagation of the onset of the bloom. It appears that the northward propagation (of the bloom onset) only concerns the subpolar spring bloom, which only exists north of approximately 40°N. The propagation speed of this bloom strongly varies with latitude and from one year to the next. It ranges between an average of 7 km/d in 2000 and 50 km/d in 2001 (the value of 20 km/d was published by *Siegel et al.* [2002]). The propagation speed of the fall bloom is also variable, around a mean of approximately 20 km/d.

[36] Figure 5b presents the times at which the ML reaches bloom-triggering values. The time when the ML shoals to a depth less than 180 m (i.e., twice the typical euphotic depth; see the discussion section 4.2) has been empirically determined to explain the restratification bloom (subpolar spring bloom). The time when the ML deepens below the nitracline depth was retained for the entrainment blooms. The nitracline depth was computed from the fall Levitus nitrate climatology, as the depth of maximum vertical gradient from the surface. As shown, the propagation of the subpolar spring bloom and its variations are rather well explained by the ML criterion. A first reason is that mixing depth is the most important limiting factor for production in this situation. A second reason is that the latitudinal propagation of solar light, which forces photosynthesis, is parallel to the propagation of the ML shoaling, and as a matter of fact, partially forces this propagation (through its contribution to Qnet).

[37] As for the entrainment bloom, the time when the ML deepens to the nitracline depth also appears to be an adequate criterion to explain the southward propagation of the bloom. Further analysis (not shown) reveals that this propagation is mainly driven by the nitracline meridional gradient (the nitracline being shallower in the north than it is in the south), and not so much by the southward propagation of the mixed layer deepening (which is much more rapid). This also suggests that interannual variability in the entrainment bloom onset and propagation is related to interannual variations in the nitrate distribution, which is absent from this analysis (Levitus climatological data had to be used for nitrate).

3.3.2.2. Bloom Strength

[38] The purpose of Figure 6 is to evaluate to what extent the bloom strength is explained by the vertical mixing intensity. For that, the mean biomass during the bloom, as a measure of its ''strength,'' is plotted against the mean MLD during the same period, as an index of vertical mixing intensity. As shown, the strength of the subpolar spring bloom (black symbols, upper line in Figure 6) and the strength of the subtropical bloom (shaded symbols with black frame, lower line) are actually correlated to the depth of the mixing, whereas no coherence emerges from a linear regression analysis for the midlatitude bloom (white symbols) and for the subpolar fall bloom (frameless shaded symbols in the bottom part of Figure 6). As expected, the restratification bloom and the entrainment bloom exhibit opposite responses. In the subpolar regime, a deeper ML (i.e., enhanced mixing) results in a weaker bloom. Indeed, the intermittent mixing events which keep perturbing the bloom might either lead to light limitation (a deeper ML further decreases the averaged light experienced by the phytoplankton cells) or simply lead to dilution. In contrast, in the subtropical regime the bloom is nutrient limited, and a deeper mean ML intensifies the bloom by increasing the nutrients input. As for the midlatitude regime, the concomitance of light and nutrient limitation forbids the emergence of a definite relationship. This competition between the two limiting factors is somewhat reflected in the distribution of

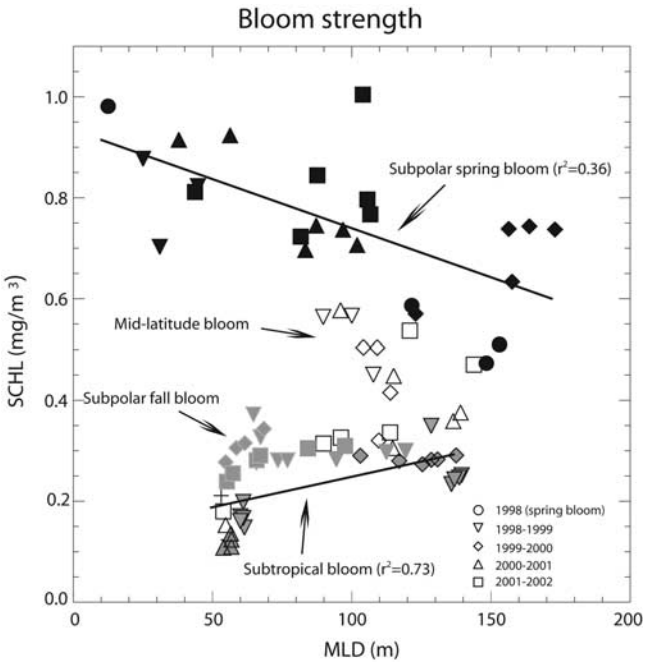

Figure 6. Mean SCHL versus mean MLD during the blooms. Solid symbols mark the subpolar spring blooms, shaded symbols with black contours mark the subtropical bloom, shaded symbols mark the subpolar fall bloom, and open symbols mark the blooms of the midlatitude regime.

the midlatitude points in Figure 6: they tend to join one or the other of the organized groups. As for the subpolar fall bloom, the point distribution looks rather parallel to the subtropical line. If no clear correlation emerges, it is likely because the bloom does not end due to the exhaustion of a nutrient pool determined by the vertical mixing during the bloom period, as it is the case for the subtropical bloom, but due to light limitation.

3.3.2.3. Regime Boundaries

[39] The interannual variations in latitude of the regime boundaries were described previously (3.3.1). In order to analyze the shift in terms of the physical forcings, the meridional variations of annual SCHL, maximum winter MLD, winter wind stress intensity and annual wind curl are plotted in Figure 7 for 1998 (black line) and 2001 (shaded line). These years were selected as extreme cases of the meridional variability in the 1998–2002 series. The meridional extension of the midlatitude regime was reported from Figure 4 for the 2 selected years (black frame for 1998, shading for 2001). For the 2 years the northern boundary of the box corresponds approximately to the same value of 0.2 mg/m^3 for the annual mean SCHL (Figure 7a) and to the same value of 250 m for the maximum winter MLD (Figure 7b) while the southern boundary corresponds approximately to 0.1 mg/m^3 and 110 m (large dots on Figure 7). This suggests that the three regimes can also be distinguished according to thresholds in annual mean biomass or maximum winter MLD.

[40] In 2001 the winter wind stress is stronger than in 1998 from 35 to 45°N (Figure 7d) and the line of zero wind stress curl (located at about 50°N) is found farther south than in 1998 (at around 55°N, Figure 7c). This is an indication of a southward shift in the northeast Atlantic wind system. Both the intergyre boundary and the ML front (Figure 7b) follow and thus the production regime boundaries. As noted before, the southward displacement of the southern boundary exceeds that of the northern limit. Indeed, an increase in wind is associated with larger heat losses, which have potentially a greater impact along the southern side where the ML is shallower than on the northern side.

4. Discussion

4.1. Methodology

[41] In order to analyze the variability of SCHL over the northeast Atlantic, 5 years of SCHL data from SeaWiFS were combined with MLDs from the Clipper ocean circulation model. This comparison revealed remarkable phase relationships in these totally independent data sets, at synoptic, seasonal and interannual timescales. A posteriori, the overall success of the MLD/SCHL comparison provides a validation of the phase of the MLD variability in Clipper. Besides, the phytoplankton bloom is influenced by other factors than the MLD, such as lateral advection [*Williams and Follows*, 1998], mesoscale activity [*Lévy et al.*, 1998; *McGillicuddy and Robinson*, 1997; *Oschlies and Garçon*, 1998], nitrogen fixation [*Michaels et al.*, 1994] and grazing [*Popova et al.*, 2002]. The relationships that nevertheless emerged between the variations in MLD and SCHL emphasize that the MLD variability is the main factor influencing the SCHL variability in that region.

[42] In order to mitigate our results, errors associated with satellite and model products are now discussed. The relatively high cloud cover in the region forces the use of 8 day composites of SeaWiFS images, in which there is a higher amount of cloud-free pixels. This filters out events of higher frequency. It also makes more difficult the comparison with model MLDs, which are an average over 5 days. Another consequence is that the precision of our timing estimates cannot be better than a week. Besides, many of our results are based on the analysis of spatial means. Owing to the nonhomogeneous character of a rather high cloud cover (twice higher in the northern part of the region than in the south), the values of meridional gradients in bloom properties have to be taken with some caution.

[43] Another uncertainty concerns the MLD absolute value estimated by the Clipper model. In order to evaluate its accuracy, a comparison was made with MLDs from three other models (Figure 8): a high-resolution (1/20°) regional model run from February to October 2001 (extension of the model run presented by *Lévy et al.* [2005]); the 1/2° resolution global configuration of OPA (http://www.lodyc.jussieu.fr/opa) and the 1/3° resolution operational model of the North Atlantic MERCATOR (http://www.mercator-ocean.fr), for the period 1998–2002. The four models are based on the same numerical code (OPA), with the same vertical mixing scheme, but with different resolutions, lateral physics, initial and boundary conditions, and forcings. The POMME model is used as a reference since its MLDs have been validated against in situ observations taken during P1 and P2 [*Lévy et al.*, 2005; *Paci et al.*, 2005]. The timing of the MLD deepenings and shallowings are the same for all models, emphasizing again the correct

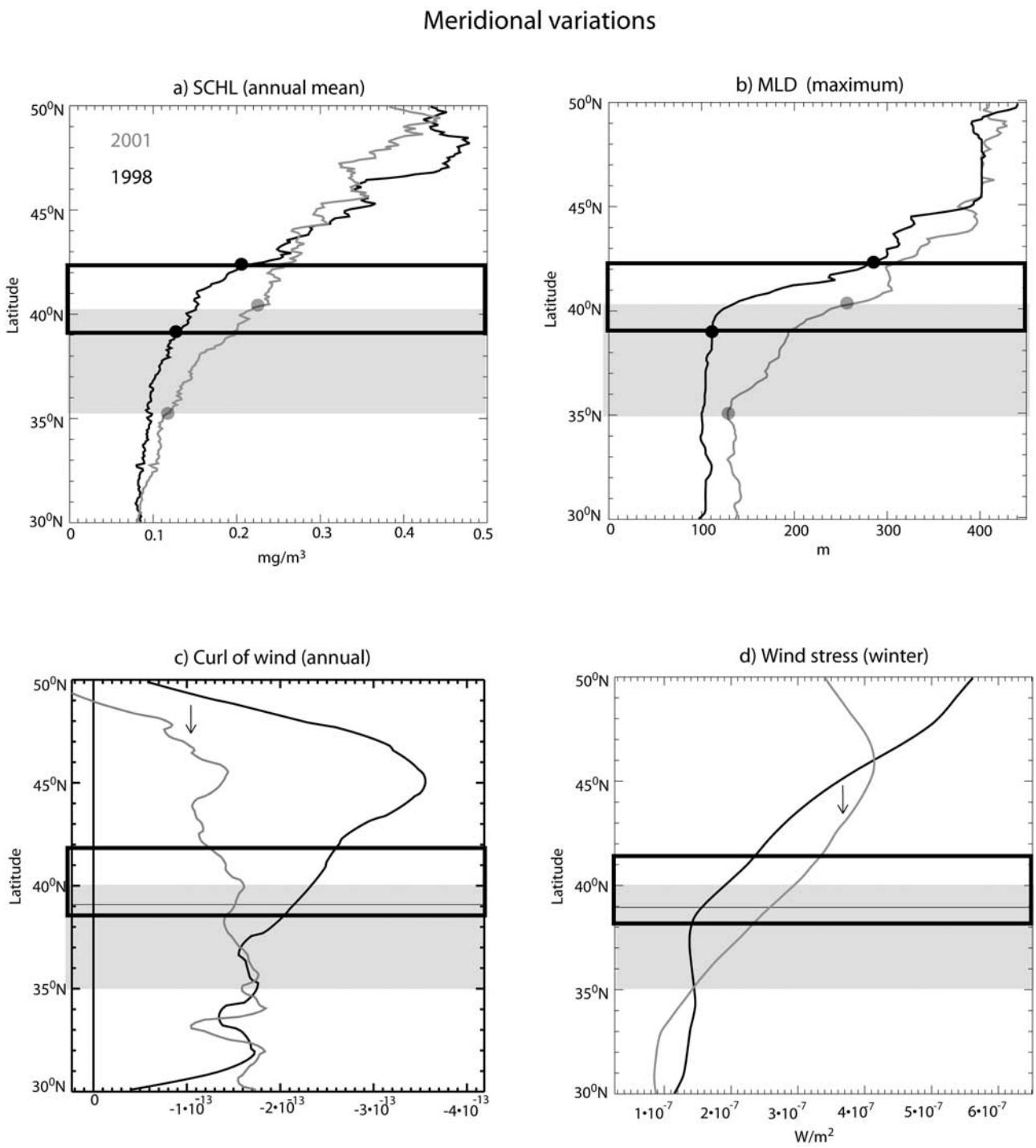

Figure 7. Meridional variations of the annual mean SCHL, the maximum annual MLD, the mean winter wind stress, and the annual mean wind curl for 1998 (black line) and 2001 (shaded line). The extension of the midlatitude region is marked with a black frame for 1998 and a shaded frame for 2001.

representation of the MLD phase (this is also true for the 4 other years; not shown). However, the MLDs amplitudes appear overestimated in Clipper, by up to 100m in March. This overestimate is due to the ECMWF heat forcing, which is too cold and not fully compensated by the SST restoring term (the best estimate annual net heat flux over POMME is 22 W/m^2 [*Caniaux et al.*, 2005], it is −10 W/m^2 in ECMWF and 6 W/m^2 in Clipper with the restoring term). In view of this overestimate, maximum MLDs from Clipper need to be corrected before attempting to derive critical values for the MLDs.

[44] Finally, the determination of regime types for each situation (Figure 4) is somewhat dependant on the data filtering prior to the application of the two criteria (section 3.3). This is however not likely to lead to worse than a 1° error in latitude when locating the boundaries.

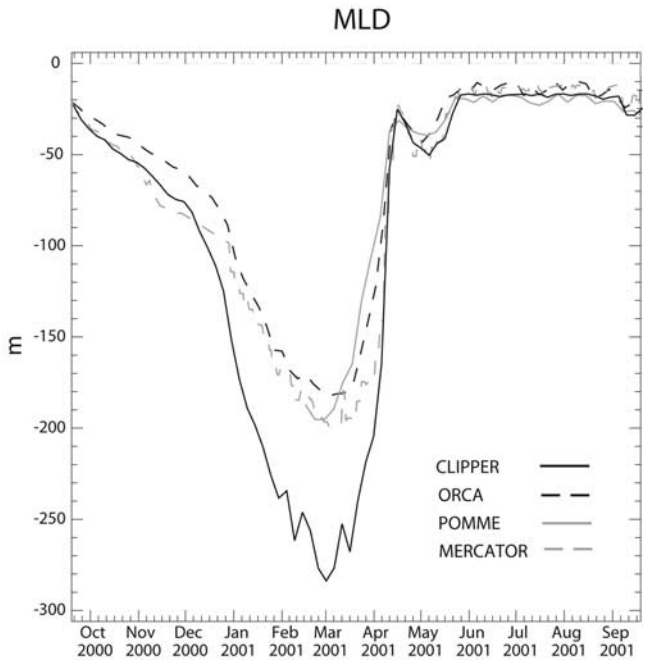

Figure 8. Time evolution of the MLD averaged over the POMME region (16°–22°W, 38°–45°N) predicted by different models from October 2000 to September 2001.

[45] Besides these technical limitations (time resolution, cloud cover, model MLDs), our approach has also inherent limitations. It only enables to address that part of the variability which is driven by vertical mixing and the biogeochemical variability is interpreted on the basis of surface (or rather ML) chlorophyll only. On the whole, comparison of fields from ocean models with satellite retrieved chlorophyll has however proven to be an interesting alternative to coupled physical-biogeochemical models for examination of the interannual variability of the production regimes, with the benefit that conclusions are not subordinated to the uncertain choice of parameterizations and parameters in the biological model.

4.2. Production Regimes

[46] Three production regimes were identified on the basis of the seasonal cycling of SCHL versus MLD. The well-known subpolar regime and subtropical regime have naturally emerged from our analysis and the data were treated with sufficient meridional resolution to emphasize a third regime, the midlatitude regime, with very specific characteristics.

[47] The characterization of the regimes presented in this work is consistent with the regime identification of *Dutkiewicz et al.* [2001], in spite of the difference in the approach. *Dutkiewicz et al.* [2001] define the subpolar and subtropical regions as the regions where enhanced mixing decreases or increases the bloom intensity, respectively. They found an intergyre region, where none of these relationships emerge. Using ocean time series observations and remote SCHL estimates from SeaWiFS, *Follows and Dutkiewicz* [2002] examine the interannual variability of the bloom intensity, in the conceptual framework of these regional regimes. Here, the regimes are defined in terms of coupled seasonal cyclings. This provides a detailed description of the characteristics of three distinct regimes. The regionalization of the regimes (Figure 4), and the relationship between bloom intensity and mixing (Figure 6), are two characteristics that emerge from the analysis of the 5 years SCHL time series.

[48] To complement the description of the regimes given for the year 2001 in section 3.2.1 and the documentation of meridional and interannual variations of their parameters given in section 3.3, a synthesis of the mean characteristics of each regime is now presented in Table 1. Basically, the regimes are organized along meridional regions. The subpolar regime is found approximately north of 41°N (±1.3°), the midlatitude regime between 36°N and 41°N and the subtropical regime south of 36°N (±2.7°). These regions correspond to different typical magnitudes of winter MLD (300 m, 150 m, and 100 m respectively). The deepest MLDs are reached around the end of February (±2 weeks), with a time shift of only 1 week between 35°N and 50°N. The annual mean SCHL in the midlatitude regime is approximately intermediate between the subpolar and subtropical regimes. The largest annual SCHL are found where winter MLDs are the deepest, and therefore where the nutrient

Table 1. Mean and Standard Deviation Characteristics of the Subpolar, Midlatitude, and Subtropical Regime Throughout the Period 1998–2002[a]

Regime	Subpolar	Midlatitude	Subtropical
Latitude range, deg	north of 41.2N ± 1.3	36.2N ± 2.7–41.2N ±1.3	south of 36.2N ± 2.7
Max annual MLD, m	310 ± 51	155 ± 32	110 ± 16
Day of maximum annual MLD	3 Mar ± 16	28 Feb ± 16	22 Feb ± 14
Mean annual SCHL, mg/m^3	0.4 ± 0.04	0.25 ± 0.07	0.15 ± 0.04
Peak of the bloom, mg/m^3		0.81 ± 0.36	0.38 ± 0.16
Fall bloom	0.44 ± 0.14		
Spring bloom	1.42 ± 0.32		
Day of bloom onset		7 Oct ± 18	29 Oct ± 26
Fall bloom	18 Sep ± 17		
Spring bloom	1 Apr ± 22		
Day of SCHL peak		4 Apr ± 25	4 Mar ± 14
Fall bloom	10 Nov ± 14		
Spring bloom	7 May ± 24		
Bloom duration, days		259 ± 15	204 ± 68
Fall bloom	117 ± 18		
Spring bloom	73 ± 22		

[a]Abbreviations are as follows: MLD, mixed layer depth; SCHL, SeaWiFS ocean color images.

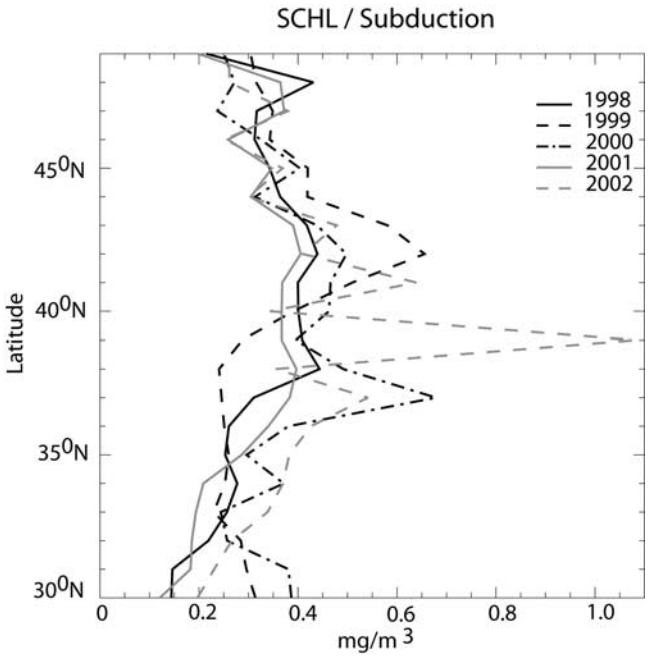

Figure 9. SCHL at the time of maximum MLD as a function of latitude for each of the 5 years.

supplies are the largest. First, this suggests that the production budget between 30°N and 50°N is primarily driven by the convective supply of nutrients, in agreement with the quantitative analysis of *Williams et al.* [2000].

[49] This suggests secondly that the seasonal cycling is strongly modulated by light limitation. At all latitudes, an entrainment bloom is initiated in fall by the deepening of the ML (from mid-September in the subpolar regime to the end of October in the subtropical regime). This bloom is more intense at midlatitudes than farther south due to the larger availability of nutrients. Traditionally, the subpolar cycling is described as the succession of an entrainment bloom in fall and an intense bloom after vernal stratification. An alternate picture of the subpolar seasonal cycling is that production is interrupted in winter (from mid-January to beginning of April) and resumes in spring. The subpolar regime is characterized by the existence of this specific winter regime, during which phytoplankton growth is inhibited by deep mixing. The subpolar winter regime does not occur in the midlatitudes and subtropics, because the ML does not get deep enough to inhibit growth. Consequently, the midlatitude bloom is the longer-lasting bloom (Table 1).

[50] Throughout the 5 years, the midlatitude regime meridional extent corresponds to relatively constant range of winter MLD (Figure 7b, from 250 m in the north to 110–140 m in the south). Although we have low confidence in these absolute values, the fact that they are consistent throughout the 5 years implies that there might be "threshold values" in winter MLD that determine the regime of a region. Following the concepts first introduced by *Sverdrup* [1953], we can derive critical values of the ratio of winter mixed layer to euphotic layer depth (Ze). Ze estimated during P1 [*Claustre et al.*, 2005] is approximately 90 m. On the basis of Figure 9, we apply a −30% correction to the Clipper winter MLDs. Coming back to Figure 7, the midlatitude regime appears now as the regime where the winter maximum MLD comprises between *Ze* and 2*Ze*. These winter conditions allow slow phytoplankton growth. In the subpolar regime, winter MLD exceeds 2*Ze*. This is too deep to allow the growth of phytoplankton. In the subtropical regime, the MLD does not get deeper than *Ze*. It is worth noting that these MLD/Ze bounds were chosen by *Lévy et al.* [1998] to parameterize the inhibition of production in situations of deep and intermediate mixing in the northwestern Mediterranean Sea.

[51] The midlatitude regime covers about half of the POMME area (the other half pertaining to the subpolar regime). This may explain some unexpected characteristics of the POMME in situ observations. The first characteristic is that in situ SCHL never exceeded 1 mgChl/m^3, even during the bloom, while higher SCHL concentrations were expected (3–4 mgChl/m^3 were observed during the North Atlantic Bloom Experiment (NABE) [*McGillicuddy et al.*, 1995]). As seen in Table 1, this value is consistent with the order of magnitude of the peak of the midlatitude bloom (0.81 ± 0.36 mgChl/m^3). Figure 4 also shows that the peak SCHL value rapidly increases with latitude above 43°N, which is consistent with the much higher values observed during NABE at 47°N. The second characteristic is that averaged primary production profiles measured during POMME (second legs of P1 and P2) clearly revealed that winter is a period of significant production, not so much different from the bloom period (37% higher primary production during spring than during winter [*Claustre et al.*, 2005]). This result was unexpected, but is less surprising in the light of the midlatitude regime concept; indeed, as mentioned before, the bloom onsets in fall in the midlatitude regime and lasts longer. The third characteristic is that the rather small *f* ratios sometimes observed during the bloom in the region (during NABE [*Garside and Garside*, 1993] and during POMME (S. Lhelguen, personal communication, 2004)) may also be explained by the fact that the bloom has actually started in winter, thus allowing the regeneration network to be fully functional by the beginning of spring.

4.3. Production in Mode Waters

[52] The production level within mode waters is of significant biogeochemical importance due to the long-term storage of surface properties subducted into deep waters. These waters are formed in winter [*Woods*, 1985] when the ML begins to retreat [*Marshall et al.*, 1993; *Hazeleger and Drijfhout*, 2000; *Valdivieso da Costa et al.*, 2005] in regions of large meridional MLD gradient [*Paillet and Arhan*, 1996a, 1996b]. For this reason, we plot in Figure 9 SCHL at the time of maximum MLD (hereafter winter SCHL) as a function of latitude. Winter SCHL is representative of the SCHL content of the water to be subducted. It is an index of the initial biogeochemical properties of the subducted waters and thus of the efficiency of the biological pump of carbon.

[53] Figure 9 shows a bowl shape structure of winter SCHL against latitude: a general feature that emerges is that winter SCHL is maximum at midlatitudes (between 35° ± 2°N and 40° ± 2°N), and minimum at high and subtropical latitudes. This singular structure ensues from the particular

properties of the midlatitude regime. Indeed, in the subpolar regime, production is weak in winter due to light limitation, and in the subtropical regime, production is always weak due to the small vertical excursion of the ML; winter production is actually optimum in the midlatitude regime. Intriguingly, the region of the midlatitude regime is the main area of subduction since it overlaps the area of maximum gradient in winter MLD (Figure 7b). This analysis therefore suggests that winter production is the highest in the region of subduction, thus reinforcing the efficiency of the biological carbon pump during subduction. Note that this result is not intuitive and relies on the particularity of the midlatitude regime. The winter MLD gradient also overlays the region of the subpolar regime (Figure 7b), but in that case winter production is weak and the pathway for carbon sequestration is thus less efficient than in the midlatitude regime.

[54] Figure 9 also suggests that the biogeochemical properties of the waters to be subducted show a large variability from one year to the next. However, this variability cannot be fully assessed without better data sets. Indeed, the difference in temporal resolution of the SCHL and MLD time series forces to interpolate the value of SCHL at the time of maximum MLD. This interpolation is uncertain, as it involves fast varying biological parameters, and may be responsible for the jagged aspect of the curves.

[55] To sum up, the midlatitude regime overlays the area of subpolar mode water subduction of the northeast Atlantic. Since subducted waters originate from the ML when the MLD is largest, the fact that the bloom starts prior to that date very likely enhances the efficiency of the biological carbon pump. Production during that period enables to convert inorganic carbon into organic form, and to sequestrate this carbon after the water mass is isolated from the influence of the atmosphere.

5. Conclusion

[56] A simple method was applied to study the variations of SCHL in relation to variations in MLD. Synoptic observations from space were found to be a valuable tool to assess the driving mechanisms of the SCHL variability over the northeast Atlantic and during POMME.

[57] This study has emphasized the large interannual variability of the production system over the northeast Atlantic, in terms of bloom timing, intensity and of the position of the geographical frontier between the various regimes. Comparison with MLD and atmospheric fields has revealed that a large part of this variability can be attributed to interannual variability in the atmosphere. At synoptic scales, the passage of storms varies from one year to another in timing and intensity. This explains why the MLD cycle is not smooth, but is punctuated by mixing events. The consequence is the different timing and intensity of the bloom, and the high frequency in SCHL. At lower frequencies, the westerlies shift from a more southerly to a more northerly track. This shift forces the shift of the winter MLD gradient (through a change in wind stress), and the location of the intergyre boundary (through a change in wind stress curl), and hence the boundaries between the biogeochemical regimes. The dominant mode of atmospheric low-frequency variability is associated with the North Atlantic Oscillation (NAO) [*Hurrell*, 1995]. *Williams et al.* [2000] have shown that the variability in nitrate supply is significantly correlated with the NAO over parts of the central and western Atlantic, but not over the eastern Atlantic. This suggests that another mode of variability may prevail in the POMME region, that still has to be elucidated, thanks to a long enough time series.

[58] After confronting our results to method limitations, they proved robust enough to support a novel interpretation of the dynamics of the North Atlantic blooms. Indeed, the midlatitude regime which emerged from our analysis fills the gap between the singular Sverdrup case and the prevalent situation of nutrient limited production. The midlatitude regime is characterized by winter MLDs in the range Ze to 2 Ze and by a bloom which evolves from autumn to spring. Besides, it covers parts of the mode water formation region. This combination likely has crucial positive impacts on the long-term carbon sequestration.

[59] The midlatitude regime needs to be further documented. Other biogeochemical parameters can be retrieved from space that should provide further insight, such as dissolved organic components (H. Loisel et al., manuscript in preparation, 2005) or phytoplankton community composition (J. Uitz et al., From surface chlorophyll a to phytoplankton community composition in oceanic waters, submitted to *Global Biogeochemical Cycles*, 2004). More sophisticated tools are needed, such as interannual coupled biological-dynamical models calibrated with the POMME data set. Their development is in the ongoing POMME project. The relationships between SCHL and MLD that emerged from this work should guide the analysis of such models.

[60] **Acknowledgments.** Financial support for this research was provided by CNES, MERCATOR, CNRS, IRD, and the PROOF program. The work of Y.L. was supported by CNES and by Tel Aviv University. We are thankful to A.-M. Tréguier, B. Barnier, J.-M. Molines, and S. Theetten for providing the outputs from the Clipper model. C. Ethé and G. Madec are acknowledged for providing the outputs from the ORCA model. We wish to thank M. Gavart for the extraction of the MERCATOR products. We thank C. de Boyer Montégut and J. Paillet for allowing the use of their data sets. M. Rafizadeh is acknowledged for his assistance in the treatment of the SeaWiFS data. Special thanks are to the Goddard Space Flight Center (GSFC/NASA) for providing the SeaWiFS images used in this work.

References

André, J. M. (1992), Ocean color remote-sensing and the subsurface vertical structure of phytoplankton pigments, *Deep Sea Res., Part A*, *39*, 763–779.

Arhan, M., A. Colin de Verdiere, and L. Mémery (1994), The eastern boundary of the subtropical North Atlantic, *J. Phys. Oceans*, *24*, 1295–1316.

Bograd, S. J., D. G. Foley, F. B. Schwing, C. Wilson, R. Michael, J. J. Polovina, E. A. Howell, and R. E. Russell (2004), On the seasonal and interannual migration of the transition zone chlorophyll front, *Geophys. Res. Lett.*, *31*, L17204, doi:10.1029/2004GL020637.

Caniaux, G., A. Brut, D. Bourras, H. Giordani, A. Paci, L. Prieur, and G. Reverdin (2005), A 1 year sea surface heat budget in the northeastern Atlantic basin during the POMME experiment: 1. Flux estimates, *J. Geophys. Res.*, *110*, C07S02, doi:10.1029/2004JC002596.

Claustre, H., M. Babin, D. Merien, J. Ras, L. Prieur, S. Dallot, O. Prasil, H. Dousova, and T. Moutin (2005), Toward a taxon-specific parameterization of bio-optical models of primary production: A case study in the North Atlantic, *J. Geophys. Res.*, *110*, C07S12, doi:10.1029/2004JC002634.

Dandonneau, Y., P.-Y. Deschamps, J.-M. Nicolas, H. Loisel, J. Blanchot, Y. Montel, F. Thieuleux, and G. Becu (2004), Seasonal and interannual variability of ocean color and composition of phytoplankton communities in the North Atlantic, equatorial Pacific and South Pacific, *Deep Sea Res., Part II*, *51*, 303–318.

de Boyer Montégut, C., G. Madec, A. S. Fischer, A. Lazar, and D. Iudicone (2004), Mixed layer depth over the global ocean: An examination of

profile data and a profile-based climatology, *J. Geophys. Res.*, *109*, C12003, doi:10.1029/2004JC002378.

Dutkiewicz, S., M. Follows, J. Marshall, and W. W. Gregg (2001), Interannual variability of phytoplankton abundances in the North Atlantic, *Deep Sea Res., Part II*, *48*, 2323–2344.

Fernández, C. I., P. Raimbault, N. Garcia, P. Rimmelin, and G. Caniaux (2005), An estimation of annual new production and carbon fluxes in the northeast Atlantic Ocean during 2001, *J. Geophys. Res.*, *110*, C07S13, doi:10.1029/2004JC002616.

Follows, M., and S. Dutkiewicz (2002), Meteorological modulation of North Atlantic spring bloom, *Deep Sea Res., Part II*, *49*, 321–344.

Garside, C., and J. C. Garside (1993), The "f-ratio" on 20W during the North Atlantic Bloom Experiment, *Deep Sea Res., Part II*, *48*, 75–90.

Hazeleger, W., and S. S. Drijfhout (2000), Eddy subduction in a model of the subtropical gyre, *J. Phys. Oceans*, *30*, 677–695.

Hurrell, J. W. (1995), Decadal trends in the North Atlantic Oscillation: Regional temperatures and precipitations, *Science*, *269*, 676–679.

Levitus, S. (1982), Climatological atlas of the world oceans, *NOAA Prof. Pap.*, *13*, 173 pp.

Lévy, M., L. Mémery, and J.-M. André (1998), Simulation of primary production and export fluxes in the northeastern Mediterranean Sea, *J. Mar. Res.*, *56*, 197–238.

Lévy, M., M. Gavart, L. Mémery, G. Caniaux, and A. Paci (2005), A four-dimensional mesoscale map of the spring bloom in the northeast Atlantic (POMME experiment): Results of a prognostic model, *J. Geophys. Res.*, *110*, C07S21, doi:10.1029/2004JC002588.

Madec, G., P. Delecluse, M. Imbard, and C. Lévy (1999), OPA 8.1 General ocean circulation model reference manual, note du pole de modelisation, 91 pp., Inst. Pierre-Simon Laplace, Paris.

Marshall, J. C., A. J. G. Nurser, and R. G. Williams (1993), Inferring the subduction rate and period over the North Atlantic, *J. Phys. Oceans*, *23*, 1315–1329.

McClain, C. R., S. R. Signorini, and J. R. Christian (2004), Subtropical gyre variability observed by ocean color satellites, *Deep Sea Res., Part II*, *51*, 281–301.

McGillicuddy, D. J., J. J. McCarthy, and A. R. Robinson (1995), Coupled physical and biological modeling of the spring bloom in the North Atlantic: (I) Model formulation and one dimensional bloom processes, *Deep Sea Res., Part I*, *42*, 1313–1357.

McGillicuddy, D. J., and A. R. Robinson (1997), Eddy-induced nutrient supply and new production in the Sargasso Sea, *Deep Sea Res., Part I*, *44*, 1427–1449.

Mémery, L., G. Reverdin, J. Paillet, and A. Oschlies (2005), Introduction to the POMME special section: Thermocline ventilation and biogeochemical tracer distribution in the northeast Atlantic Ocean and impact of mesoscale dynamics, *J. Geophys. Res.*, doi:10.1029/2005JC002976, in press.

Menzel, D. W., and J. H. Ryther (1961), Annual variations in primary production in the Sargasso Sea off Bermuda, *Deep Sea Res.*, *7*, 282–288.

Michaels, A. F., and A. H. Knap (1996), Overview of the US JGOFS Bermuda Atlantic time-series study and Hydrostation "S" program, *Deep Sea Res., Part II*, *43*, 157–198.

Michaels, A. F., et al. (1994), Seasonal patterns of ocean biogeochemistry at the US JGOFS Bermuda Atlantic Time-series Study site, *Deep Sea Res., Part I*, *41*, 1013–1038.

Michaels, A. F., D. Alson, J. L. Sarmiento, J. W. Ammerman, K. Fanning, R. Jahnke, A. H. Knap, F. Lipschultz, and F. Prospero (1996), Inputs, losses and transformations of nitrogen and phosphorus in the pelagic North Atlantic, in *Nitrogen Cycling in the North Atlantic Ocean and Its Watersheds*, edited by R. W. Howarth, pp. 181–226, Springer, New York.

Oschlies, A., and V. Garçon (1998), Eddy-induced enhancement of primary production in a model of the North Atlantic Ocean, *Nature*, *394*, 266–269.

Paci, A., G. Caniaux, M. Gavart, H. Giordani, M. Lévy, L. Prieur, and G. Reverdin (2005), A high-resolution simulation of the ocean during the POMME experiment: Simulation results and comparison with observations, *J. Geophys. Res.*, doi:10.1029/2004JC002712, in press.

Paillet, J., and M. Arhan (1996a), Shallow pycnoclines and mode water subduction in the eastern North Atlantic, *J. Phys. Oceans*, *26*, 96–114.

Paillet, J., and M. Arhan (1996b), Oceanic ventilation in the eastern North Atlantic, *J. Phys. Oceans*, *26*, 2036–2052.

Paillet, J., and H. Mercier (1997), An inverse model of the eastern North Atlantic general circulation and thermocline ventilation, *Deep Sea Res., Part I*, *44*, 1293–1328.

Popova, E. E., C. J. Lozano, M. A. Srokosz, M. J. R. Fasham, P. J. Haley, and A. R. Robinson (2002), Coupled 3D physical and biological modelling of the mesoscale variability observed in North-East Atlantic in spring 1997: Biological processes, *Deep Sea Res., Part I*, *49*, 1741–1768.

Sathyendranath, S., R. S. A. Longhrst, C. M. Caverhill, and T. Platt (1995), Regionally and seasonally differentiated primary production in the North Atlantic, *Deep Sea Res., Part I*, *38*, 355–377.

Siegel, D. A., S. C. Doney, and J. A. Yoder (2002), The North Atlantic spring phytoplankton bloom and Sverdrup's critical depth hypothesis, *Science*, *296*, 730–733.

Stramska, M., T. D. Dicky, A. Plueddemann, R. Weller, C. Langdom, and J. Marra (1995), Bio-optical variability associated with phytoplankton dynamics in the North Atlantic Ocean during spring and summer of 1991, *J. Geophys. Res.*, *100*, 6621–6632.

Sverdrup, H. U. (1953), On conditions for the vernal blooming of phytoplankton, *J. Conseil*, *18*, 287–295.

Tréguier, A. M., O. Boebel, B. Barnier, and G. Medec (2003), Agulhas eddy fluxes in a 1/60 Atlantic model, *Deep Sea Res., Part II*, *50*, 251–280.

Valdivieso da Costa, M., H. Marcier, and A.-M. Treguier (2005), Effects of the mixed layer time variability on kinematic subduction rate diagnostics, *J. Phys. Oceanogr.*, *4*, 427–443.

Williams, R. G., and M. J. Follows (1998), The Ekman transfer of nutrients and maintenance of new production over the North Atlantic, *Deep Sea Res., Part I*, *45*, 461–489.

Williams, R. G., and M. J. Follows (2003), Physical transport of nutrients and the maintenance of biological production, in *Ocean Biogeochemistry: The Role of the Ocean Carbon Cycle in Global Change*, edited by M. Fasham, pp. 19–51, Springer, New York.

Williams, R. G., A. J. McLaren, and M. J. Follows (2000), Estimating the convective supply of nitrate and implied variability in export production over the North Atlantic, *Global Biogeochem. Cycles*, *14*, 1299–1313.

Woods, J. D. (1985), The physics of the thermocline ventilation, in *Coupled Ocean-Atmosphere Models*, pp. 543–590, Elsevier, New York.

Yoder, J. A., C. R. McLain, G. C. Feldman, and W. E. Esaias (1993), Annual cycles of phytoplankton chlorophyll concentrations in the global ocean: A satellite view, *Global Biogeochem. Cycles*, *7*, 181–193.

J.-M. André, Institut Pierre-Simon Laplace/Institut de Recherche Pour le Développment, 4, place Jussieu, F-75252 Paris Cedex 05, France. (andre@lodyc.jussieu.fr)

E. Heifetz, Geophysics and Planetary Sciences, Tel Aviv University, Tel Aviv 69978, Israel. (eyalh@cyclone.tau.ac.il)

Y. Lehahn and M. Lévy, Institut Pierre-Simon Laplace, Centre National de Recherche Scientifique, 4, place Jussieu, F-75252 Paris Cedex 05, France. (yllod@lodyc.jussieu.fr; marina.levy@lodyc.jussieu.fr)

H. Loisel, Laboratoire d'Optique Atmosphérique, Universite des Sciences et Technologies de Lille, F-59655 Villeneuve d'Ascq, France. (loisel@loa.univ-lille1.fr)

L. Mémery, Laboratoire des Sciences de l'Environnement Marin/Institut Universitaire Européen de la Mer, Centre National de Recherche Scientifique, Technopole Brest Iroise, F-29280 Plouzané, France. (memery@lodyc.jussieu.fr)

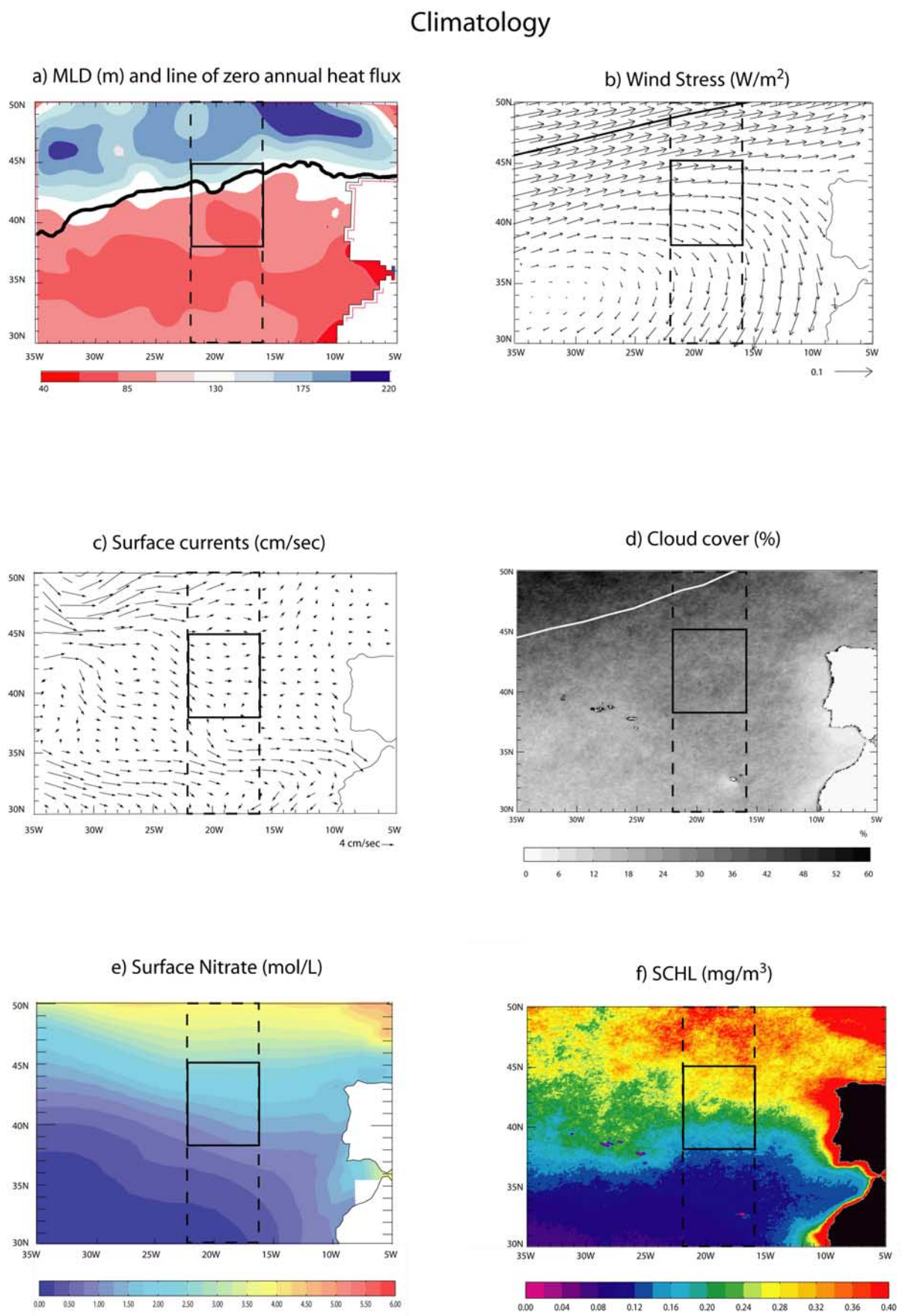
Climatology
a) MLD (m) and line of zero annual heat flux
b) Wind Stress (W/m2)
c) Surface currents (cm/sec)
d) Cloud cover (%)
e) Surface Nitrate (mol/L)
f) SCHL (mg/m3)
50N
45N
40N
35N
30N
35W
30W
25W
20W
15W
10W
5W
40
85
130
175
220
0.1
4 cm/sec
%
0
6
12
18
24
30
36
42
48
52
60
0.00
0.50
1.00
1.50
2.00
2.50
3.00
3.50
4.00
4.50
5.00
5.50
6.00
0.00
0.04
0.08
0.12
0.16
0.20
0.24
0.28
0.32
0.36
0.40

Figure 1

Figure 1. A climatological view of the northeast Atlantic. (a) Winter mixed layer depth (MLD) (after *de Boyer Montegut et al.* [2004]) and the line of zero annual net heat flux in Clipper between the years 1998 and 2002. (b) Wind stress (European Centre for Medium-Range Weather Forecasts (ECMWF)) and line of zero wind stress curl. (c) Surface currents (after *Paillet and Mercier* [1997]). (d) Cloud cover as percent of flag occurrence over 1998–2002 in Sea-viewing Wide Field-of-view Sensor (SeaWiFS) weekly chlorophyll products (see text) and the line of 50% cloud cover. (e) Surface nitrate [*Levitus*, 1982]. (f) Surface chlorophyll (average of SeaWiFS ocean color images (SCHL) over 1998–2002). The solid frame marks the Programme Océan Multidisciplinaire Méso Echelle (POMME) region, and the dashed frame marks the region examined in the present study.

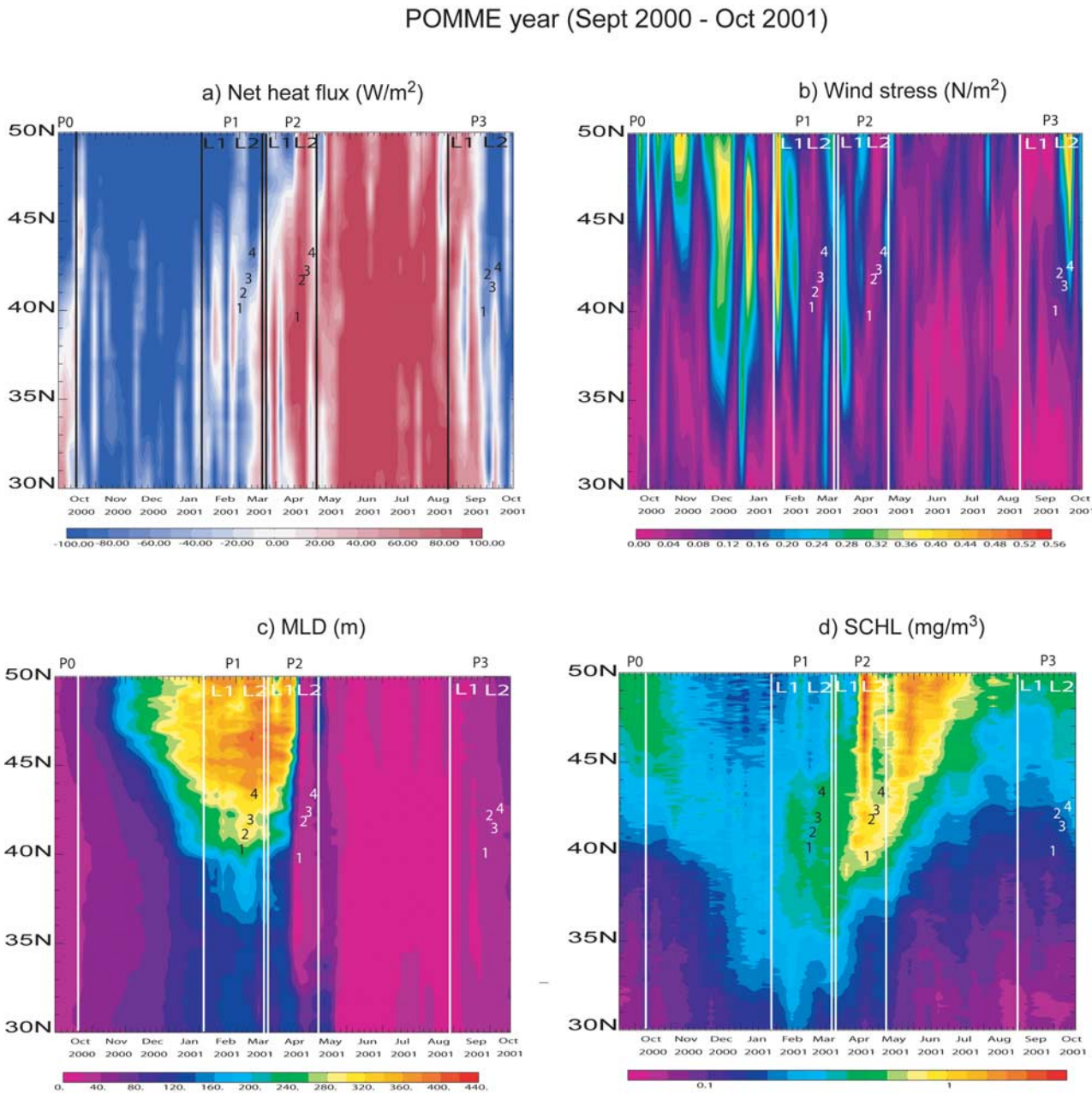

Figure 2. Temporal and meridional variations of zonal averages (16°–22°W) from September 2000 to October 2001 of (a) net heat flux (Clipper), (b) wind stress (ECMWF), (c) MLD (Clipper), and (d) SCHL (SeaWiFS). The vertical lines mark the period of each POMME survey (P0 to P3). The numbers mark the location and time of the time series stations. Legs 1 (L1) and 2 (L2) of each survey are also indicated.